Accepted Manuscript

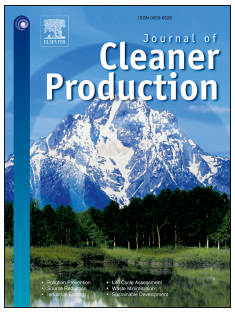

Palm oil kernel shell as solid fuel for the commercial and industrial sector in Ecuador: tax incentive impact and performance of a prototype burner

Mario A. Heredia Salgado, Luís A.C. Tarelho, M. Arlindo A. Matos, Daniel Rivadeneira, Ricardo A. Narváez C

PII: S0959-6526(18)33842-3

DOI: https://doi.org/10.1016/j.jclepro.2018.12.133

Reference: JCLP 15191

To appear in: *Journal of Cleaner Production*

Received Date: 26 April 2018

Revised Date: 10 December 2018

Accepted Date: 13 December 2018

Please cite this article as: Mario A. Heredia Salgado, Luís A.C. Tarelho, M. Arlindo A. Matos, Daniel Rivadeneira, Ricardo A. Narváez C, Palm oil kernel shell as solid fuel for the commercial and industrial sector in Ecuador: tax incentive impact and performance of a prototype burner, *Journal of Cleaner Production* (2018), doi: 10.1016/j.jclepro.2018.12.133

Palm oil kernel shell as solid fuel for the commercial and industrial sector in Ecuador: tax incentive impact and performance of a prototype burner

Mario A. Heredia Salgado[a], Luís A.C Tarelho[a], M. Arlindo A. Matos[a], Daniel Rivadeneira[b], Ricardo A. Narváez C[b]

[a] Department of Environment and Planning, Centre for Environmental and Marine Studies (CESAM), University of Aveiro, 3810-193, Portugal
[b] Instituto Nacional de Eficiencia Energética y Energías Renovables (INER), EC170507 Quito-Ecuador.

*Corresponding author: heredia.mario@ua.pt (Mario A. Heredia Salgado)

Abstract

The Ecuadorian industrial and commercial sectors are in general supported in the use of diesel for energy purposes. An alternative to replace diesel could be the use of palm oil residual biomass as solid fuel. It is estimated that 57.7% of the capital costs required to implement a biomass boiler that use KS as fuel in replacement of a diesel boiler would be covered by in force tax incentives. Nonetheless, untaxed and subsidized diesel utilization coupled to the important capital and operating costs associated to the biomass boiler results in relatively high payback periods, within the range of 6 to 7.9 years. Analyzing a base case, it is observed that replacement of diesel by untreated palm oil kernel shell (KS) results in a reduction of 8 times the fuel costs. Implementation of pre-treatment processes (e.g. pelletizing) could increase the KS price, affecting the potential to lower the costs of thermal energy production. Accordingly, utilization of raw KS to thermal energy production was demonstrated using a horizontal burner prototype. The experimental analysis of the KS combustion process shows that combustion efficiency (99.8%) is as high as that observed in other type of biomass burners. During the steady state operation periods, CO concentration in the flue gases (260.1 mg/Nm^3) was below the limit established by the European standards for solid fuel boilers (500 mg/Nm^3). Ash sintering was observed in the grate during the combustion experiments. The ash discharge process induced periodic fluctuations in the combustion chamber temperature profile as well as fluctuations in the flue gas composition. Despite these localized and periodic temperature and gas composition fluctuations, in the whole, and considering longer periods of operation, the combustion system was under steady state conditions and showed to be suitable for energetic valorization of untreated KS.

Keywords

Biomass combustion; Palm oil residual biomass; Subsidies; Agriculture fuels; Tax incentives; Horizontal burner

1. Introduction

In Ecuador, the high liquid fuels demand is a major concern. The use of liquid fuels of fossil origin namely: diesel (31%), gasoline (28%), fuel oil (8%), LPG (8%) and kerosene (3%), represent 78% of the energy consumed in the country (Castillo et al., 2017). Diesel represents almost half (42%) of the overall liquid fuels demand (Villada et al., 2016). Although the fact that diesel is mostly consumed in the transportation sector, it is also consumed in the industrial and commercial sectors to produce thermal energy (Instituto Nacional de Eficiencia Energética y Energías Renovables, 2018). It has been estimated that 41.4% of the diesel and 89.5% of the fuel oil used for thermal energy production in the Ecuadorian industrial and commercial sectors could be replaced by biomass derived solid fuels (Mitschke, 2016). However, the introduction of biomass derived solid fuels in Ecuador has been limited by the in force domestic energy policy that subsidize fossil fuels consumption (Heredia et al., 2018). There is a price rate that differentiate large-scale and small-scale industrial consumers according to the volume of diesel consumed (Presidencia de la República, 2015). The industrial or commercial consumers that require less than 2000 diesel gallons per month pay a subsidized price of 0.90 USD/gal. Meanwhile, consumers that require more than 2000 gallons per month pay a diesel price that does not consider any subsidy (2.02 USD/gal) (PETROECUADOR, 2018). Besides subsidies, there are not specific taxes applied for large scale or small-scale diesel consumers, except the value added tax (12%). As a consequence, diesel price in Ecuador is one of the lowest in South America (Mendoza, 2014).

Considering that low energy prices have been driven the consumption of oil derived fuels, the Ecuadorian government implemented a group of tax incentives to promote the introduction of alternative energy sources. The Organic Law of Internal Tax Regime (Honorable Congreso Nacional, 2014) considers two major tax incentives for the implementation of renewable energy systems: a) a depreciation rate of 100% (rather than the traditional 10%) for the companies that voluntarily acquire equipment's, machines and technology for renewable energy production and b) a five year income tax payment exemption for the companies that make new and productive investments in the renewable energy sector. The influence of

these tax incentives on the financial performance of an energy system that aims to replace diesel by a biomass derived solid fuel is still unknown, and for that reason analysis of this subject is of major importance to be studied.

The current status of the palm oil agroindustry in Ecuador is characterized by the production of a significant quantity of residual biomass. It is estimated that residual biomass production is around twice the amount of crude palm oil produced (Garcia-Nunez et al., 2016). Accordingly, its proper treatment and final disposition is major environmental and economic concern (Garcia-Nunez et al., 2015b). Recognition of the serious environmental impacts associated to palm oil production led to the emergence of the Roundtable on Sustainable Palm Oil (RSPO) (Danielsen et al., 2009; Koh and Wilcove, 2008). The principles and criteria of the RSPO are ambitious sustainability standards to prevent environmental and social impacts associated to palm oil production (Roundtable on Sustainable Palm Oil, 2013). Accordingly, the RSPO has brought attention to the potential uses of the residual biomass generated in the mills, since it can be converted through the use of different technologies (cogeneration, pyrolysis, gasification, etc.) into value-added products (Garcia-Nunez et al., 2015a).

An alternative to replace subsidized diesel and reduce liquid fuels demand in the Ecuadorian industrial sector could be the use of biomass derived solid fuels provided by the palm oil mills. Ecuador is the second largest palm oil producer in South America (Ministerio de Agricultura Ganadería Pesca y Acuacultura, 2014). In Ecuador, palm oil crops and mills are mainly concentrated in the lower flanks of the Andes mountain range, at typical altitudes of 600 m.a.s.l. (see Figure 1). The palm oil crop is not seasonal, thus residual biomass is continuously produced in the mills. Currently, the Ecuadorian palm oil sector generates $6.9x10^9$ kg/y of residual biomass, namely: a) empty fruit bunches (EFB) ($5x10^8$ kg/y), b) mesocarp fibers (MF) ($3.1x10^8$ kg/y), c) kernel shells (KS) ($1.2x10^8$ kg/y) and d) field wastes (FW) ($5.9x10^9$ kg/y) (Ministerio de Electricidad y Energía Renovable, 2014). Accordingly, the Ecuadorian palm oil sector can ensure a constant supply of residual biomass derived fuels along the year.

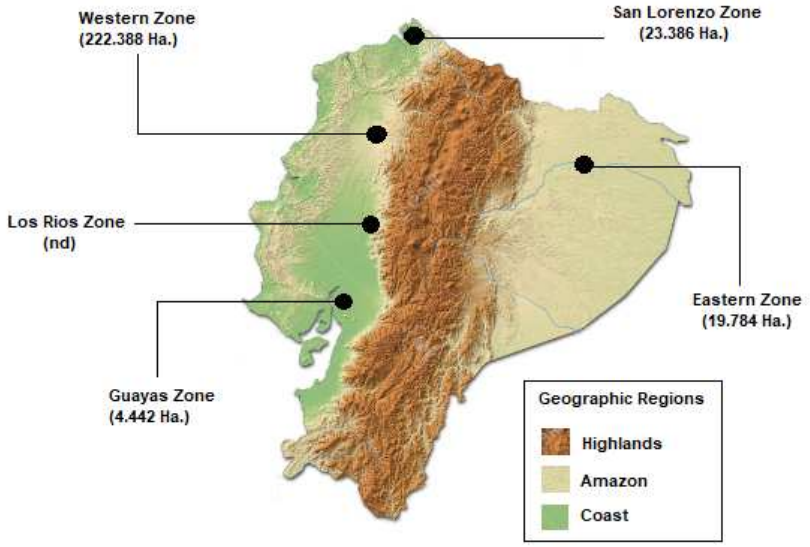

Figure 1. Geographical location of the palm oil sector in Ecuador. Palm oil plantation census 2013 (nd – not determined) (Ministerio de Agricultura Ganadería Pesca y Acuacultura, 2014)

Comparatively to EFB, MF and FW, the KS is preferred for energetic applications because its lower moisture content (11 wt%), lower ash content (5.2 wt%) and higher bulk density (1.12 g/cm^3) (Dagwa. and Ibhadode., 2008; Vassilev et al., 2010). The reported combustion efficiency in fluidized bed reactors using KS as fuel (particle diameter of 5mm) is between 99.4-99.7% under excess air of 40-50%, (Ninduangdee. and Kuprianov., 2014). KS combustion experiments using fluidized bed and batch reactors report the effects in flue gas composition, flame front speed and burning rate resulting from increasing the excess air rate up to 80% (Razuan et al., 2010). However, the use of KS to replace diesel for thermal energy production in the Ecuadorian highlands (cities located at typical altitudes above 2000 m.a.s.l) may require to increase the excess air rate above 100%. To the best knowledge of the authors, there is no information about the effects in the KS combustion process efficiency as a result of using the high excess air rates required to compensate the decrease in O_2 concentration in the air observed in the highlands. Unlike information on the use of fluidized bed and batch reactors, experimental evidence is scarce on the adaptation of other type of burners for KS combustion, for example, horizontal flame burners. Thus, a proper identification of the combustion efficiency and flue gas composition under the referred altitude

conditions (typical altitudes above 2000 m.a.s.l) using horizontal flame burners is of most relevance in the field.

The technical implications of using KS as fuel in the Ecuadorian highlands and the existence of tax incentives for implementation of biomass valorization infrastructure's require an integrated techno-economic analysis. Accordingly, this manuscript performs a financial assessment aiming to identify potential policy limitations or market restrictions for the introduction of KS as fuel for thermal energy production. Complementarily, the effects of altitude conditions in the KS combustion process are also studied using a horizontal burner prototype developed to experimentally demonstrate the KS combustion process. The combustion experiments were performed at an altitude of 2635 m.a.s.l. and the observed flue gas composition was used to assess the combustion efficiency according to the European eco-design requirements for solid fuel industrial boilers.

2. Materials and Methods

The analysis of the KS potential to replace diesel during thermal energy production in the Ecuadorian highlands was divided into two major components: a) a financial assessment and b) an experimental assessment. For the financial assessment, the study considers field data from a municipal recreational and sport complex located in the Ecuadorian highlands that currently uses a diesel boiler to heat a semi-olympic pool and produce hot water. The proposed alternative considers the replacement of the diesel boiler by a biomass boiler using KS as fuel, however, keeping the diesel boiler as a backup and emergency system. Typical operating and capital costs of biomass combustion systems are used to estimate the main financial performance indexes. Further, total tax burden and tax benefits associated to the use of KS as fuel for thermal energy production were calculated.

For the experimental assessment, a horizontal biomass burner prototype was developed and constructed to analyze and demonstrate the combustion process of untreated KS. All the experiments were performed at typical altitude of cities located in Ecuadorian highlands (2635 m.a.s.l.). Modifications in the

stoichiometry of the combustion process in result of the altitude considered were calculated through a numerical model. Temperature profile in the combustion chamber and temperature distribution in relation to the flame length were monitored using K-type thermocouples and open source hardware and software platforms. Finally, the flue gas composition was monitored during the combustion experiments and CO_2 and CO concentration in the flue gases were used to calculate the combustion efficiency according to the European eco-design requirements for solid fuel industrial boilers (The European Commission, 2015a). Details of the financial and numerical models including a description of the experimental infrastructure used to analyze the use of KS as solid fuel for thermal energy production in the Ecuadorian highlands are presented in the following sections.

2.1. RETScreen model: base case

Field data were collected from a municipal recreational and sport complex that owns a semi-olympic pool (L×W= 25m×15m). The pool water is maintained at 33°C throughout the year. The thermal energy required in a yearly basis to heat the pool and for hot water service (showers) was estimated using RETScreen® software. The climate database considered for simulation corresponds to a city in the Ecuadorian highlands (latitude: °N -1.2, longitude: °E -78.6). The climate database estimates an average annual room temperature of 16.8°C, an average annual relative humidity of 71%, and an average annual solar radiation of 4.3 kWh/m^2/d. The calculation method 2 was defined for RETScreen® simulation and LHV was used as reference heating value in the software. The model considers an indoor type pool and the use of a pool cover during nights (9 h/d). The pool area was estimated in 375 m^2 and makeup water percentage was set in 10%. The pool load profile was set in 100% during summer season (June-August) and 90% during the rest of the year. For the hot water service (showers), the estimated water consumption was set in 0.3 (m^3/d); the daily hot water temperature was set in 33°C and 6 days of operation per week were considered. The fuel used for the base case analysis was diesel. Diesel density and LHV considered were 833 kg/m^3 at 15 °C and 43.4 MJ/kg (The engineering toolbox, 2018a). The diesel CO_2 emission factor was estimated in 3.2 kg_{CO2}/kg_{diesel}. The diesel price was differentiated between subsidized (0.90

USD/gal) and un-subsidized price (2.02 USD/gal) (PETROECUADOR, 2018). Regarding the units used in this manuscript, only diesel fuel consumption will be presented in the unit USA gallons rather than international unit m^3, because the domestic policy refers the unit USA gallons (1 gal = 3.79 l) to establish the difference between subsidized and unsubsidized diesel price.

2.2. Cost structure and financial performance model

Smaller energy conversion systems have substantially higher costs per unit of installed capacity than large energy conversion systems (Nilsson et al., 2011). Table 1 shows the cost structure used to analyze the financial performance of a bioenergy system that uses KS as fuel to produce thermal energy considering that the resulting energy system will be even below the defined small-scale threshold of 2000 t/y (Shackley et al., 2011).

Table 1. Cost structure used to assess the financial performance of a combustion system using KS as fuel to produce thermal energy.

	Cost	**Reference**
Operational costs	(USD/t)	
Biomass feedstock cost	27	(Mitschke, 2016)
Specific operation and maintenance costs	12.46*	(Shackley et al., 2011)
Initial investment costs	(USD/kW_{th})	
Boiler	197.71*	(Carbon Trust, 2009)
Fuel feeding system	27.08*	(Carbon Trust, 2009)
Fuel storage	58.23*	(Carbon Trust, 2009)
Boiler house	138.13*	(Carbon Trust, 2009)
Accumulator	8.13*	(Carbon Trust, 2009)
Flue gas system	21.67*	(Carbon Trust, 2009)
Design, PM, commissioning	28.44*	(Carbon Trust, 2009)

Transport/delivery	9.48*	(Carbon Trust, 2009)
Pipes and fittings	5.42*	(Carbon Trust, 2009)
Wiring and control	12.19*	(Carbon Trust, 2009)

*Exchange rate 1GBP = 1.35 USD

The overall cost of the system C was defined in a yearly basis through Eq. (1) as the sum of initial investment costs I_0 and operational costs OC (see Table 1).

$$C = I_0 + OC \quad (1)$$

The net cash flow CF was estimated in a yearly basis according to Eq. (2) considering as revenues: a) the savings S_f due to diesel replacement by KS and b) the revenues due to trading of CO_2 avoided emissions S_{CO2} assuming a price of 15 USD/t_{CO2} (Shackley et al., 2011). Finally, operational costs OC (see Table 1) were considered as cash outgoings.

$$CF = S_f + S_{CO2} - OC \quad (2)$$

The simple payback period PP was estimated through Eq. (3) by the relation between the system overall costs C over the project years, and the net cash flow CF. The project life time was assumed to be 20 years.

$$PP = \frac{C}{CF} \quad (3)$$

The operating income OI was calculated through Eq. (4) to assess the influence of the preferential depreciation rate considered for the implementation of residual biomass valorization infrastructures according to the Organic Law of Internal Tax Regime (Honorable Congreso Nacional, 2014). Hence, the depreciation rate D_c in Eq. (4) was assessed between the preferential rate of 100% and the typical depreciation rate of 10%.

$$OI = CF - D_c \quad (4)$$

Ecuador considers two main taxes for companies: the income tax and the profit sharing tax. The Organic Law of Internal Tax Regime (Honorable Congreso Nacional, 2014) considers a five year income tax exemption for the implementation of residual biomass valorization infrastructures. The income tax I_t is usually calculated over the free cash flow index FCF. Hence, FCF is calculated according to Eq. (5) considering the I_t as zero during the first five years and 22% for the rest of the project lifetime.

$$FCF = OI \cdot (1 - I_t) \tag{5}$$

Finally, to consider the total tax burden associated to the proposed bioenergy system, the earnings before taxes and depreciation ($EBTD$) index was estimated through Eq. (6). $EBTD$ calculation considers a profit sharing tax Ps_t of 15% over the FCF according to the Ecuadorian Labor Code (Honorable Congreso Nacional, 2016).

$$EBTD = FCF \cdot (1 - Ps_t) \tag{6}$$

2.3. Numerical model for KS combustion in high-altitude conditions

The numerical model developed to define the stoichiometry of the combustion process in high-altitude conditions considers the proximal and elemental composition of KS. In Ecuador, some palm oil mills add salt to the extraction process to promote separation between the oil nut and the shell. In these cases, KS contains salts which represent a major concern in relation to its later use as fuel. The KS samples taken from the field for determining the proximal and elemental composition and for the combustion experiments do not contain additional salts from the extraction process. The methods used to determine the KS elemental and proximal composition are shown in Table 2.

Table 2. List of methods used to perform the proximate and elemental analysis of palm oil kernel shell. The kernel shell samples taken from the field does not have salts.

Parameter	Method
Moisture	BS EN 14774-3:2009

Ash	BS EN 14775:2009
Volatile matter	BS EN 15148:2009
Heating value	ASTM D 1989-96
C, H, N, S	BS EN 15104:2011

According to the elemental composition of KS, the stoichiometric O_2 consumption W_s was calculated through Eq. (7).

$$W_s = Y_{s,C} \cdot \left(\frac{W_{C,F}}{M_C}\right) + Y_{s,H} \cdot \left(\frac{W_{H,F}}{M_H}\right) + Y_{s,S} \cdot \left(\frac{W_{S,F}}{M_S}\right) - \left(\frac{W_{O,F}}{M_O}\right) \quad (7)$$

The atmospheric air was considered as source of O_2 for the combustion process. Thus, the stoichiometric air consumption $W_{s,a}$ was estimated through Eq. (8). For calculation purposes, it was estimated as representative of average values for combustion air, the values of 13.9 °C and 10% for temperature and relative humidity. It should be noted that for $W_{s,a}$ calculation, the O_2 concentration in the air in high-altitude locations is lower than 21%vol. From to the ideal gas law, the volume that 0.21 Kmol of O_2 occupy at PTN conditions is 4.7 m^3 (air temperature of 273.1 K, air pressure of 101325 Pa, and a R value of 8314.5 J/kmol·K). Thus, considering the same volume of 4.7 m^3, but correcting the atmospheric pressure to 75300 Pa (The engineering toolbox, 2018b) corresponding to the considered altitude conditions, the resulting O_2 molar concentration is 0.16 Kmol. Accordingly, the stoichiometric coefficients ($Y_{s,O}$, $Y_{s,N}$ and Y_{H2O}) used in Eq. (8) were adapted to a O_2 molar concentration of 0.16 Kmol.

$$W_{s,a} = W_s \cdot \left(Y_{s,O} + \left(Y_{s,N} \cdot \frac{M_N}{M_O}\right) + \left(Y_{H2O} \cdot \frac{M_{H2O}}{M_O}\right)\right) \quad (8)$$

The actual air $W_{a,A}$ was estimated according to Eq. (9) by adjusting the excess air rate z in order to have an oxygen concentration of 8-10%vol dry gas in the exit flue gas, according to conditions observed during combustion in typical biomass furnaces (Carvalho et al., 2018; Obaidullah et al., 2014).

$$W_{a,A} = (1 + z) \cdot W_{s,a} \quad (9)$$

The stoichiometric ratio (lambda λ index) was estimated through Eq. (10).

$$\lambda = \frac{W_{a,A}}{W_{s,a}} \quad (10)$$

Finally, the global mass balance equation used to estimate the theoretical flue gas composition is shown in Eq. (11).

$$\left(\frac{W_{C,F}}{M_C}, \frac{W_{H,F}}{M_H}, \frac{W_{O,F}}{M_O}, \frac{W_{N,F}}{M_N}, \frac{W_{S,F}}{M_S}, \frac{W_{W,F}}{M_W}, W_{Z,F}\right) + \left(\frac{W_{a,A}}{M_{air}}\right) \cdot (W_{s,a}) = \left(n_{CO2} + n_{H2O} + n_{O2} + n_{SO2} + n_{N2} + \frac{W_{Z,F}}{12}\right) \quad (11)$$

2.4. Experimental infrastructure

The combustion experiments were performed in a geographical location at 2635 m.a.s.l. corresponding to the coordinates: S0°17'30.8" W78°30'7.9". A 30 kW_{th} horizontal burner prototype was developed to demonstrate the combustion process of residual biomass. The biomass fuel used in the combustion experiments was untreated KS with a particle diameter between 6-10 mm (irregular bowl like chip of 5 mm thick). Each combustion experiment lasted 9 hours that includes the heating stage and the stationary state periods. The burner is a cylindrical fixed bed type (D×L = 15cm × 13.5 cm) that integrates an automatic ash discharge system. The layout of the horizontal burner prototype is shown in Figure 2.

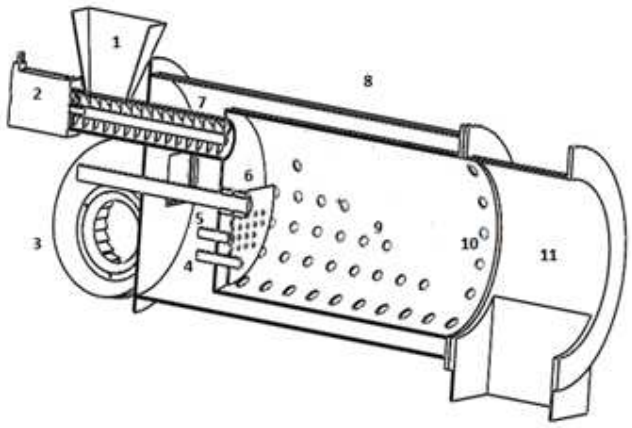

Figure 2. General schematic of the horizontal burner prototype used in the combustion experiments. Legend: 1. Biomass hopper, 2. Biomass feeder, 3. Blower, 4. Electric heater for ignition, 5. Infrared flame sensor, 6. Ash discharge system, 7. Feeding system, 8. Burner frame, 9. Combustion bed, 10. Secondary air and flame stabilization boreholes ring, 11. Ash discharge port.

The burner main parameters and peripheral devices for power control are managed and monitored by an open source hardware and software microcontroller board (Arduino MEGA 2560 LLC, Italy). The visual interface between user and the Arduino microcontroller board is performed through a 4.3 inch TFT LCD display. All these systems were embedded in a control box. The horizontal burner prototype ignition system uses an electric heater of 200W (item 4 in Figure 2) to heat the combustion air and start the combustion process until the flame front is stabilized. The ignition system is used only during the startup of the combustion experiments. The combustion air during the initial ignition and combustion processes is supplied by an electric blower (item 3 in Figure 2) which speed is controlled from the Arduino microcontroller board. The resulting air mass flow according to the blower speed was monitored by an extra Arduino UNO microcontroller board integrated to: a) a pitot tube, b) a MPXV7002 differential pressure sensor (Sensitivity 1.0 V/kPa; 2.5% typical error over +10°C to +60°C.) and c) a 16×2 LCD display for data visualization. The primary air is supplied through 34 boreholes of 5 mm diameter each, distributed in a delta configuration over the grate of the combustion bed (item 9 in Figure 2). The

secondary air is supplied through 23 boreholes of 5mm diameter each, placed in a ring arrangement at the biomass burner exit (see item 10 in Figure 2). This ring arrangement is also used for flame stabilization. The biomass is transported from the burner hopper (item 1 in Figure 2) to the combustion bed by a horizontal spring feeder type system (item 7 in Figure 2). The speed of the feeder motor (item 2 in Figure 2) is also controlled and monitored from the Arduino microcontroller board. The spring feeder system was choose to be implemented because it was observed that during KS transport, strength and hardness of the biomass particles requires elastic deformation of the transporting system. The spring feeder dimensions are: 3.5 cm in diameter and 36.5 cm length, spring thickness 0.5 cm and spring pitch 3.3 cm. The mass flow curve of the feeder system in relation to the feeder motor speed was defined using an electronic scale (resolution: 1 g). The automatic ash discharge system is timed driven and consists of an axle of axial movement attached to a vertical flat blade that displace the ash bed towards the burner front (see item 6 in Figure 2). The ash discharge system is driven by a planetary gearbox stepper motor controlled by the Arduino microcontroller board. When the ashes reach the biomass burner exit, they follow down through an ash discharge port of 15cm width × 13cm length (see item 11 in Figure 2). The ash discharge port resembles a “T” fitting and has a locking valve to prevent air entrance. The Arduino microcontroller board that controls the horizontal burner prototype establishes serial communication with a computer interface in order to plot, monitor and record all the burner related data in real time, namely: state of the ignition system, activation period of the ash discharge system, mass flow of combustion air and KS mass flow.

For the combustion experiments, the horizontal burner prototype is coupled to a cylindrical combustion chamber (D×L= 0.65m × 1.7m) with a 15 cm thick thermal insulation layer (see Figure 3). The combustion chamber has a heat exchange device that is not analyzed in this work. Therefore, the effective volume of the combustion chamber is 0.44 m^3. The temperature profile in the combustion chamber was monitored using K-type thermocouples attached to MAX6675 boards synchronized and monitored by an additional Arduino UNO microcontroller board. The temperature data logger is connected by serial

communication to a computer interface in order to plot, monitor and record temperature data in real time. Thermocouples location is show in Figure 3. The flue gas composition (dry gas: CO, CO_2, HC and O_2) was monitored through an AU Mobile Brain Bee infrared on line analyzer. For safety reasons a particle matter filter followed by a gas condenser submerged in cold water for moisture and condensable material removal were placed before the gas analyzer. The gas analyzer establishes communication with the data acquisition system by Bluetooth, to visualize, plot and record the flue gas composition data. A general schematic of the horizontal burner prototype, the combustion chamber and the data monitoring and acquisition devices is shown in Figure 3.

In the absence of an Ecuadorian emissions regulation for small-scale combustion systems, the CO emissions were assessed according to the implementing directive of the European Parliament with regard to eco-design requirements for solid fuel boilers (The European Commission, 2015b). Accordingly, the CO concentration values are expressed at normalized conditions of pressure (101.3 kPa) and temperature (273.15 K) in mg/Nm^3 and corrected to a concentration of 11%vol O_2 dry gas in the flue gas according to Eq. (12) (MAMAOT, 2013).

$$CO_{corr} = \frac{(O_{2\,air} - O_{2\,ref})}{(O_{2\,air} - O_{2\,fg})} \cdot CO_{actual} \tag{12}$$

Where: $O_{2\,air}$ is the O_2 concentration in the atmospheric air (%vol), $O_{2\,ref}$ is the reference O_2 concentration (11%vol according to the eco-design requirements for solid fuel boilers), $O_{2\,fg}$ is the monitored O_2 concentration in the flue gas and CO_{actual} is the monitored CO concentration in the flue gas (mg/Nm^3). All concentrations are referred to dry gas. Finally the efficiency of the combustion process (CE) was calculated through the Eq. (13) (Loo and Koppejan, 2008). The CO_2, CO values in Eq. (13) are expressed in %vol, dry gas.

$$CE = \frac{CO_2}{(CO_2 + CO)} \cdot 100 \tag{13}$$

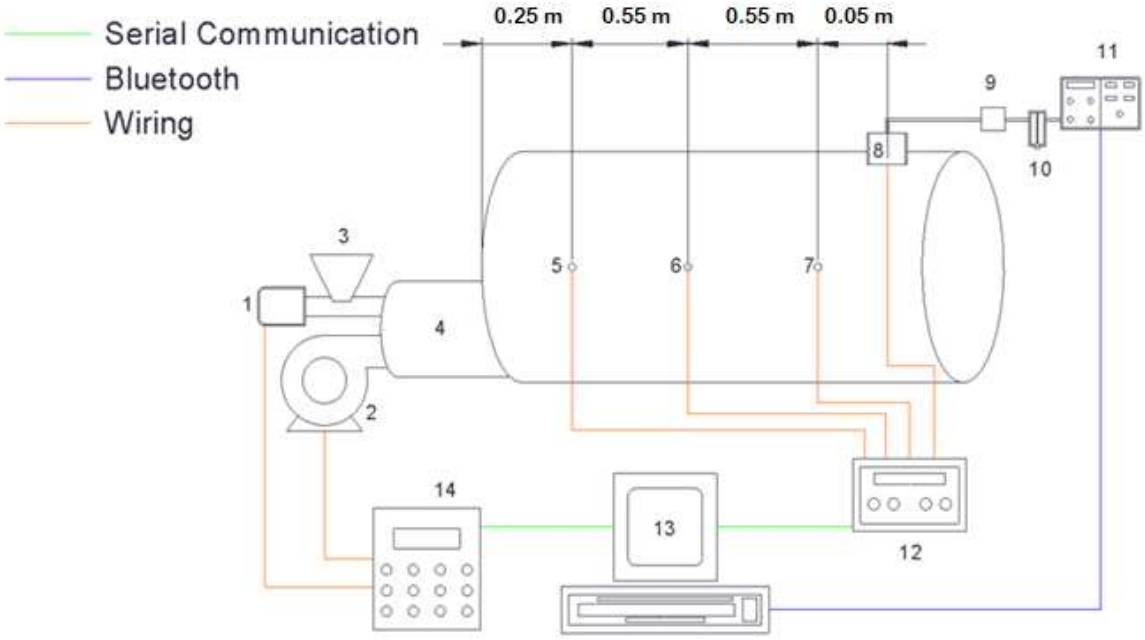

Figure 3. General schematic of the horizontal burner prototype coupled to the combustion chamber, electronic controls, monitoring devices and data acquisition systems. Legend: 1. Biomass feeder, 2. Blower, 3. Biomass hopper, 4. Burner frame, 5. Thermocouple T1, 6. Thermocouple T2, 7. Thermocouple T3, 8. Thermocouple T4, 9. Particle filter, 10. Condenser filter, 11. On line gas analyzer, 12. Thermocouple data logger, 13. Data acquisition, 14. Biomass burner electronic control.

In another setup arrangement (see scheme in Figure 4), the biomass burner was coupled to a flanged pipe (D×L= 0.15m × 1.25m) with a 15 cm thick thermal insulation layer to study the combustion gas temperature in relation to the flame length and its relation to the air excess ratio. These combustion experiments lasted 60 minutes. The thermocouples location (K-type) is show in Figure 4.

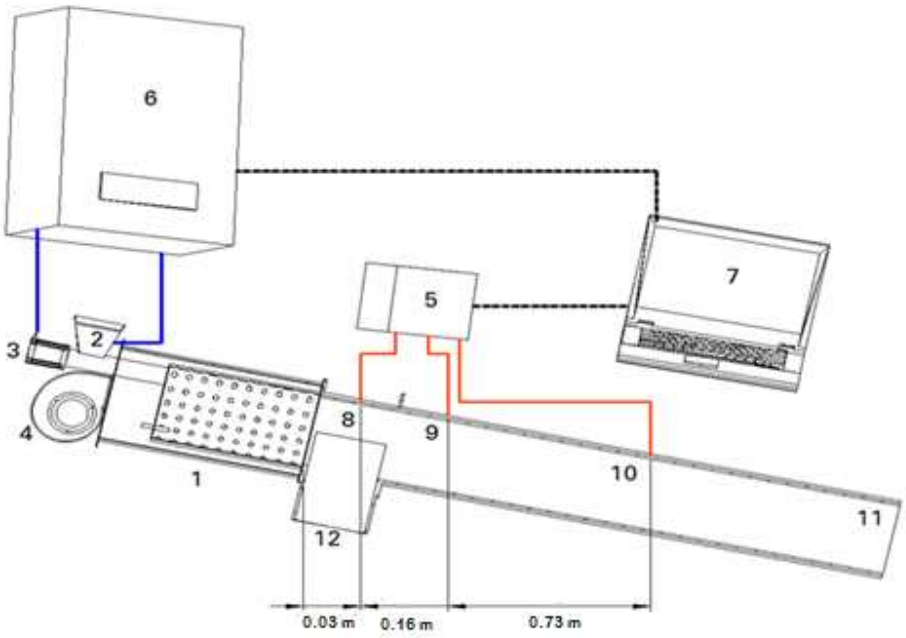

Figure 4. General schematic of the experimental infrastructure used to estimate the gas temperature in relation to the flame length and its relation to the excess air ratio. 1. Burner frame, 2. Biomass hopper, 3. Biomass feeder, 4. Blower, 5. Thermocouple data logger 6. Burner electronic control, 7. Data acquisition, 8. Thermocouple 1, 9. Thermocouple 2, 10. Thermocouple 3 11. Insulated flanged pipe 12. Ash discharge port.

3. Results and discussion

3.1. Financial assessment

According to the RETScreen® simulation, the thermal power of a boiler intended to heat the pool and produce the required hot water (see base case in Section 2.1) is 250 kW_{th}. The resulting energy consumption according to the load profile would be of 918 MWh/y. To provide this energy, the annual fuel consumption would be 24175.4 diesel gallons which is equivalent to 220.3 tons of KS. Table 3 shows the annual fuel cost associated to the pool heating and hot water, considering the fuel consumption pattern above referred. The fuel costs result from the annual fuel consumption multiplied by the price of each of the two energy vectors considered. The KS price considered was 27 USD/t (see Table 1). The diesel price considers two cases, unsubsidized price of 2.02 USD/gal and subsidized price of 0.90 USD/gal.

Consideration of unsubsidized price over subsidized price depends on whether the monthly consumption limit exceeds 2000 gallons per month.

Table 3. Financial analysis of a thermal energy production system that aims the replacement of a diesel boiler by a biomass boiler that use untreated KS as fuel.

Financial analysis	
Fuel costs (USD/y)	
Unsubsidized diesel	48834.2 ([a])
Subsidized diesel	21757.8 ([b])
Untreated kernel shell	5948.6 ([c])
Financial performance indexes	
PP (y)	7.9
CF (USD/y)	37855.3
OI (USD/y)	31523.3
FCF (USD/y)	24588.2
$EBTD$ (USD/y)	20899.9
Tax burden (USD/y)	
Income tax	6935.1
Profit sharing tax	3688.2
Tax Incentive (USD)[(d)]	
Five year income tax exemption (USD) (22% over the *FCF*)	34675.6
Preferential depreciation rate (USD/y) (100% rather than typical 10%)	1920.5

[a] Diesel cost does not consider subsidy:2.02 USD/gal ((PETROECUADOR, 2018)

[b] Diesel cost consider subsidy: 0.90 USD/gal ((PETROECUADOR, 2018)

[c] KS price according to the cost structure of Table 1

[d] Tax incentives estimated through Eq. (4) and (5) according to the Organic Law of Internal Tax Regime (Honorable Congreso Nacional, 2014)

It is observed that using KS in replacement of unsubsidized diesel (2.02 USD/gal), results in a reduction of 8 times the fuel cost (see Table 3). Likewise, the use of KS in replacement of subsidized diesel (0.90 USD/gal) results in a fuel cost reduction of 3.6 times. The KS price considered in this analysis (27 USD/t) takes into account a transportation fee of 10 USD/t and does not include any pre-treatment processes as drying or pelletizing (see Table 1). Pelletization of biomass fuels (as for example KS) is often claimed as an alternative to improve fuel properties and decrease transportation costs. In Ecuador the price of a pelletized biomass fuel has been estimated in a range between 110 USD/t and 180 USD/t depending on the feedstock (Mitschke, 2016). For the analyzed base case, the use of a pelletized fuel (e.g, KS) with a price that starts from 110 USD/t, would make the use of biomass derived solid fuels more expensive than using subsidized diesel. It is stated that the price increase in the pelletized fuel would be compensated by a significant reduction in the transportation cost due to the increase in the fuel density. This assertion may not be applicable to the analyzed case, because there are not major differences between density of untreated KS (1.12 g/cm^3) and the one of a standard pelletized biomass fuel (1.15 g/cm^3) (Dagwa. and Ibhadode., 2008; Pio et al., 2017).

Considering the base case of Section 2.1, the capital cost required to replace the diesel boiler by a biomass boiler is 126664.6 USD with an operating cost of 8693.8 USD/y. If the fuel cost is reduced by 8 times, the payback period (*PP*) to recover the overall investment is 7.9 years (see Table 3). Despite the evident reduction in the fuel costs, the replacement of the diesel boiler by a biomass boiler is associated to significant initial investment and also important operating costs, accordingly the payback period (*PP*) is relatively high. Overestimation of the operational and capital costs may be influencing the *PP* index, as these values were taken from literature (USA and UK). Nevertheless, similar analysis using analogous cost structures shows that typical *PP* for biomass based thermal energy production systems is 2.9 years in the case of wood chips and 4.7 years in the case of pellets (Carbon Trust, 2009). It was found that the

major distortion between the analyzed case and other *PP* of biomass based thermal energy production systems reported in literature (e.g. Carbon Trust, 2009) is related to the low diesel price in Ecuador. In turn, the low diesel price is a result of the current subsidies policy to fossil fuels and the absence of specific taxes on their consumption.

According to Table 3, the tax incentives that apply for the replacement of a diesel boiler by a biomass boiler equals to an amount of 73085.5 USD which represents 57.7% of the initial investment costs. The tax incentives that promote the use of alternative energy sources result of adding the preferential depreciation rate and the 5 year income tax exemption. It is observed that the *PP* decrease from 7.9 to 6 years as a result of discounting the amount correspondent to tax incentives from the initial investment costs (i.e. from 126664.6 USD to 53579.1 USD). However, a 6 year *PP* index, is still higher than those observed (e.g. Carbon Trust, 2009) in the case of wood chips (2.9 years) and pellets (4.7 years).

3.2. Experimental assessment

From the financial analysis (see Section 3.1), it is observed that replacement of diesel by KS produce a significant reduction of fuel costs. The KS price (27 USD/t) is competitive even considering that diesel can be purchased with no major taxes and with subsidies involved. As show in Section 3.1, the use of other biomass fuels with a price higher than 27 USD/t, for instance pelletized fuels (e.g., 110 USD/t), could turn financial unfeasible the introduction of biomass derived fuels in replacement of diesel. Hence, it is important to develop energy conversion equipment's able to process the available fuel (untreated KS) avoiding pre-treatment processes that would increase the fuel costs. Likewise, optimization of the capital cost associated to those energy conversion devices is required to improve the *PP* index. In this context, the experimental analysis made here includes the use of a low cost horizontal burner prototype (see Section 2.4) to study the limitations potentially associated to the combustion process of raw (untreated) agro-residual biomass, the KS, that could be used as fuel in Ecuador. The proximate and elemental composition of the KS taken from the field and used in the combustion experiments is show in Table 4.

Table 4. Proximate and elemental analysis (methods in Table 2) of raw (untreated) KS taken from the field and used as fuel in the combustion experiments.

	Palm oil Kernel Shell (KS)
Proximate Analysis (%wt,$_{wb}$)	
Moisture	5.4
Ash	1.8
Elemental Analysis (%wt,$_{db}$)	
Ash	1.9
C	51.6
H	6.0
N	[a]
S	1.2
O	39.3[b]
Higher Heating Value - HHV (MJ/kg$_{db}$)	19.5

[a] Bellow the detection limit (100 ppm)
[b] Calculated by difference

In relation to the typical KS proximal and elemental analysis reported in literature (Chin et al., 2015; Masiá et al., 2007; Uemura et al., 2011; Vassilev et al., 2010), the KS samples used in this work show a higher sulfur content and lower ash content (see Table 4). The high sulfur and low ash content in the analyzed KS samples could be related to soil conditions during plant growing, as well as fertilizers utilization. Nonetheless, the KS ash content is still 2 times higher than a standardized pelletized fuel (Pio et al., 2017). High ash content in the feedstock and high combustion temperatures will produce slags as

well as sticky ash particles that promote fouling in heat transfer surfaces (Zeng et al., 2016) and prevent proper combustion air distribution in the grate even being able to promote flame extinguish. The use of residual biomass with high ash content, as KS, may give rise to molten phases during combustion if the ash melting temperature is exceeded. The combustion temperature is influenced by the combustion process stoichiometry. In turn, combustion process stoichiometry is strongly influenced by altitude conditions. At an altitude of 2634 m.a.s.l., this study estimates a decrease in the O_2 concentration in the air (from 21 $\%_{vol}$ to 16$\%_{vol}$) as a result of the atmospheric pressure decrease (see Section 2.3). Accordingly, the excess air rate has to be amended to values between 100% and 170% to reach the typical O_2 concentration in the flue gas observed during residual biomass combustion, that is, 8 to 10$\%_{dry\ gas}$. Figure 5 shows the combustion gases temperature at different locations of the flame length along the biomass burner, considering excess air rates of 100% and 170%. The data shown in Figure 5 follows the combustion experiments performed according to the experimental infrastructure shown in Figure 4.

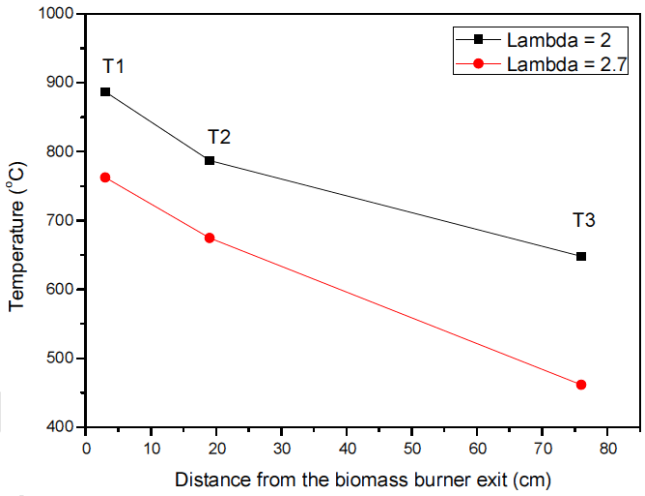

Figure 5. Influence of the excess air rate in the temperature of combustion gases at different locations of the flame length along the biomass burner. Fuel: untreated KS. Stoichiometric conditions: λ= 2 and 2.7

It is observed that combustion gases temperature decreases as the distance from the biomass burner exit increases (Figure 5). This is explained by the heat exchange between hot flame gases and the surrounding

environment. According to Figure 5, for λ= 2 equivalent to 100% of excess air, the higher axial temperature observed in the flame region is 886.8°C. The highest axial temperature is found at the thermocouple 1 location, immediately after the flame stabilization ring and secondary air supply. A lambda increase from 2 to 2.7, i.e. an increase in the excess air rate from 100% to 170%, causes a decrease of the higher temperature in the flame region from 886.8°C to 762.4°C, at thermocouple 1 location (see Figure 5). Any increase in the excess air rate to compensate the decrease in the oxygen concentration in the combustion air due to altitude conditions produces a considerable decrease in the combustion temperature. This effect of the increasing excess air in lowering the flame temperature is well known (Loo and Koppejan, 2008) and is related to a higher ratio between the amount of combustion flue gases to be heated (and N_2 diluted) and the fuel feed rate.

It has been stated that combustion temperatures higher than 700 °C can result in strongly sintered ashes, while combustion temperatures higher than 800 °C results in molten ashes (Chin et al., 2015), although those phenomena are influenced by ash composition (Zeng et al., 2018). Considering the temperatures observed in the flame region in this work (Figure 5), it can be expected that some problems of ash sintering and melting can occur in the horizontal burner prototype (see Figure 2). Combustion experiments using the experimental infrastructure shown in Figure 3, with 9 hours duration were performed to assess the short term combustion system performance and possible ash related problems.

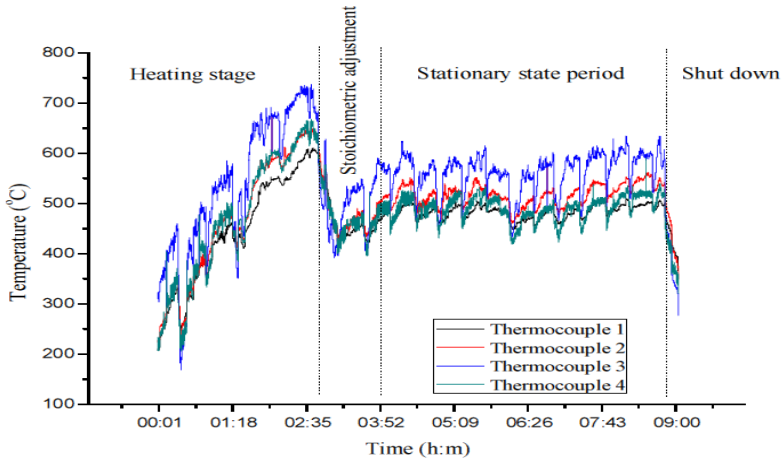

Figure 6. Axial temperature profile in the combustion chamber corresponding to each stage of the combustion experiments. Location of the thermocouples in the combustion chamber is shown in Figure 1

The combustion experiments were divided into four stages: a) heating, b) stoichiometric adjustment, c) stationary state period and d) shut down (see Figure 6). The heating stage includes the startup of the horizontal burner prototype, the flame stabilization process and the steady state operation process at a power of 27 kW_{th} (KS feed rate: 8.5 kg/h). After the heating stage, the horizontal burner prototype power was decreased to a more stable condition of 23 kW_{th} (KS feed rate: 7.2 kg/h). The decrease of the burner power produces a decrease in the combustion chamber temperature (see stoichiometric adjustment stage in Figure 6). After this stoichiometric adjustment, a stationary state period of operation is observed. The stages of the combustion experiments are characterized by fluctuations in the temperature profile along time in the combustion chamber. The temperature fluctuations of lesser amplitude are related to irregularities in the biomass feeding, mainly resulting from the heterogeneous physical-chemical properties of KS, e.g. particle size (6-10 mm), and this is a common behavior observed in biomass combustion systems (e.g., (Tarelho et al., 2015). The temperature fluctuations of greater amplitude are related to the activation time of the automatic ash discharge system (every 25 minutes). It was observed that once the combustion process has started, a layer of sintered ash is accumulating at the bottom of the biomass combustion bed in the burner. The KS particles fed and entering the combustion region of the burner begin to be thermally decomposed over this ash layer. After 25 minutes, there is an increase in the thickness of the ash layer formed at the combustion bed, preventing a proper feed of KS particles to the combustion region of the burner. Ash accumulation in the combustion bed required the development of a proper operating device and procedure for automatic ash removal in order to maintain the combustion process (see Section 2.4). he automatic ash discharge system developed pushes forward the ash bed in order to enable a proper feeding of KS particles. The activation of the ash discharge system guarantees the maintenance of adequate conditions for the combustion process in the burner and discharges the excess ash. This movement of solids, ash and burning KS particles, is the responsible for the major temperature fluctuations observed in Figure 6. These major temperature fluctuations are explained by the transition of

a bed of ash and KS particles burning, to new feed of KS particles that enter to the combustion bed. The major temperature fluctuations are also related to the ignition process of the newly fed KS particles, which is preceded by two major endothermic sub-processes, namely: initial heating accompanied by drying and initial steps of biomass devolatilization (Calvo et al., 2014). This explains the temperature decrease in the combustion chamber in the period subsequent to the activation of the ash discharge system; that is, a consequence of thermal energy consumption in the initial endothermal processes of heating, drying and devolatilization. Despite this localized and periodic temperature and gas composition fluctuations, in the whole, and considering longer periods of operation, the combustion system is under steady state operation conditions.

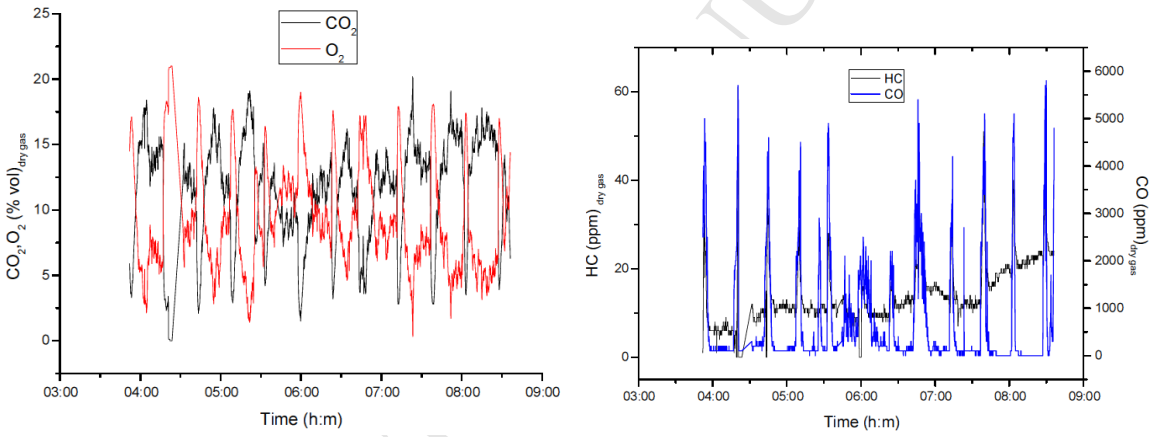

Figure 7. Exit flue gas composition during the steady state period of the KS combustion process. CO_2 and O_2 concentrations presented in %vol and CO and HC concentration presented in ppm, both in a dry gas volume basis

During the stationary operation, the periodic and automatic ash discharge process and ignition of newly fed KS particles to the combustion bed produces a decrease in the CO_2 concentration in the flue gas, and an increase in the O_2 concentration every 25 minutes (see Figure 7). This fluctuation is related to discharging the ash bed and the initial stages of conversion (heating, drying and devolatilization) of newly fed KS particles. As the flow rate of combustion air fed to the biomass burner does not change during the ash discharge process (the blower speed is constant during the steady-state period), there is a high excess air in the combustion reactor at this time event. The low temperature in this stage and poor mixing

between combustion air and the volatile species being released during the ignition process of the new KS particles entering the combustion bed produce a peak in the CO and HC concentration in the combustion flue gas that repeats cyclically (every 25 min) as observed in Figure 7. This increase in the CO and HC concentration is accompanied by a decrease in the CO_2 concentration and an increase in the O_2 concentration in the flue gas. The HC and CO concentration peaks are related to the release of volatiles (pyrolytic process) of the newly feed KS particles that enter the combustion bed and start to be thermally decomposed. At this stage, besides the existence of O_2 in excess, the relatively low temperature observed (see Figure 6) coupled to some poor gas mixing in the burner causes an inefficient conversion of the combustible pyrolysis gases and thus, relatively high concentrations of CO and in minor amount, unburned hydrocarbons (HC). From Figure 7, it is observed that ignition process of the newly KS particles after the automatic discharge of the ashes, has an average duration of 4.4 minutes. In the period between 5h:37 min and 6h:37 min in Figure 7, the ignition period is slightly longer, and the CO peaks are lower. This phenomenon is caused by the ash fall down through the ash discharge port placed between the burner and the combustion chamber (see Figure 2). The ash discharge port was implemented to facilitate the ash extraction and as an attempt to adapt the horizontal burner prototype to conventional heat exchange devices currently integrated to diesel or gas burners. The ash removal process in the biomass burner is a complex process that results in periodic localized perturbations in the combustion system, and sometimes in unwanted shut down events. This unwanted shutdown events occur when large sintered ash pieces drag the combustion bed while falling through the ash discharge port. Ash clogging in the ash discharge port was also observed in some experiments.

After activation of the ash discharge system, the average CO concentration in the exit flue gas is 4877.8 mg/Nm^3 (corrected to a reference value of 11% O_2, dry gases), that is higher than the emission limit established by the European standards for solid fuel boilers (500 mg/Nm^3, at 11% O_2, dry gases). However, the periods of steady state combustion (each has an average duration of 21.6 minutes) prevails over the ash discharge periods, and newly fed KS particles ignition periods (4.4 minutes). The steady state

combustion periods occur under an excess air rate of 100%, equivalent to $\lambda = 2$. The observed O_2 concentration in the flue gas during the steady state combustion periods is in average 8%vol $_{dry\ gas}$, and thus, in accordance to the typical value observed during biomass combustion (Carvalho et al., 2018; Obaidullah et al., 2014). Likewise, the average CO concentration observed during the periods of steady state combustion (260.1 mg/Nm^3), corrected to a reference value of 11% O_2, dry gases, is below the emission limit (500 mg/Nm^3, at 11% O_2, dry gases) established by the European standards for solid fuel boilers. During the periods of steady-state combustion, the average combustion efficiency is 99.8%, while during the periods subsequent to the activation of the ash discharge system the average combustion efficiency decreases to the range 93.4% to 96.9% (see Eq. 13).

The high ash content of the KS fuel and its management in the combustion system is the main reason for the observed decrease in the combustion efficiency in the periods subsequent to the activation of the ash discharge system. Combustion of biomass with high ash content, as the agro-residues (e.g., KS), is a challenge that requires an optimized burner operation. Combustion bed temperatures higher than 700°C should be avoided to prevent ash sintering problems. Moreover, the strategies of staged combustion and further advanced air staging techniques could be alternatives to prevent both pollutant emissions and ash related problems (Amand et al., 2001). The use sub-stoichiometric regimes could re-locate the high temperature zones away from the combustion bed, where the ash sintering problems become evident. Other alternatives to increase the available combustion time for the KS energy conversion in the burner could be the implementation of fuel pre-treatment processes. Leaching by acetic acid solutions or even water could effectively remove the ash forming elements and thus increase the ash melting temperature (Chin et al., 2015). Nevertheless, special attention should be paid to the increase in the KS cost due to the implementation of these type of pre-treatment processes, because any increase in the KS price to more than 110 USD/t could turn the biomass fuel more expensive than diesel in the present Ecuadorian scenario (see Section 3.1).

4. Conclusions

The use of untreated palm oil kernel shell (KS) as fuel could contribute to reduce the consumption of diesel currently used to produce thermal energy in the Ecuadorian industrial and commercial sectors. The in force tax incentives that promote the integration of renewable energy sources would cover 57.7% of the capital costs required to replace a diesel boiler by a biomass boiler to use KS as fuel. However, the payback period is still relatively high (6 to 7.9 years) due to the high capital and operating costs associated to the biomass boiler and the subsidized and tax-free consumption of diesel.

The fuel costs of a thermal energy production system that uses diesel (2.02 USD/gal, unsubsidized price) could be 8 times lower when using untreated kernel shell (KS) as fuel. Even considering the lower diesel price (0.92 USD/gal, subsidized), the fuel cost of the thermal energy production system could be reduced 3.6 times by using of KS as fuel. The calculation of the fuel cost reduction considers a KS price of 17 USD/t and a transportation fee of 10 USD/t. Any pre-treatment processes, for instance pelletizing, may increase the KS price from 27 USD/t to 110 USD/t, turning biomass utilization more expensive than diesel. To keep low KS fuel prices and still achieve a significant fuel costs reduction, pre-treatment processes should be avoided as far as possible. Considering a scenario of no changes in the present Ecuadorian energy policy (i.e., subsidized and untaxed diesel consumption maintained), capital costs reduction related to the biomass valorization infrastructure, operating costs optimization and KS utilization in raw form are major alternatives identified to make feasible the use of KS as fuel in the Ecuadorian industrial and commercial sector.

The experimental assessment shows the adequacy of the developed horizontal burner prototype as a cost effective solution to use raw KS as fuel for thermal energy production. Despite heterogeneity in the particle size of the KS used in the experiments (diameter: 6-10mm), the combustion process efficiency (99.8%) is as higher as that observed in other works using the same fuel in batch and fluidized bed reactors (99.4 – 99.7%). The calculated combustion efficiency (99.8%) occurs under O_2 concentration in the flue gas of 8%vol, that is a typical operating condition observed during residual biomass combustion. The excess air rate required to reach the referred condition was 100%. It was observed that an increase in

excess air rate from 100% to 170% produces a considerable flame quenching effect decreasing the higher combustion temperature from 887°C to 762°C. During the steady-state periods the observed CO concentration (260.1 mg/Nm^3 at 11% O_2, dry gases) in the exit flue gases was well below the emission limits established by the European standards and the eco-design requirements for solid fuel industrial boilers (500 mg/Nm^3 at 11% O_2, dry gases). The activation of the ash discharge system resulted in high CO concentration (4877.8 mg/Nm^3) in the flue gases. During the ash discharge procedure the combustion efficiency decreases to values around 93.4 - 96.9%, and this is related to poor combustion conditions during the initial decomposition stages (endothermic processes as heating, drying and devolatilization) of the newly fed KS particles entering the burner´s bed after the activation of the ash discharge system. Thus, further research to improve the operation of the developed prototype of combustion system must be made in order to optimize the existing ash management within the burner. Among the options are included the implementation of advanced air staging techniques to decrease the combustion bed temperature and prevent ash melting in the grate. Ash sinterization avoidance would decrease the periodic time required to remove the ashes from the burner and will also facilitate the feeding of newly KS particles to the combustion bed. In turn, temperature and flue gas composition fluctuations could be attenuated. Although previous studies show that pre-treatment of the agro-residues, e.g., by leaching method, can reduce the ash content and increase the ash fusibility temperature, thus contributing to minimize the ash related problems observed here with KS, this pre-treatment will increase KS price reducing its potential to compete with current diesel prices, and thus should be subject of further study.

Acknowledgements

This work was supported by the *Instituto de Fomento al Talento Humano*-IFTH and The Republic of Ecuador. It is acknowledged the support to CESAM - Centre for Environmental and Marine Studies, POCI-01-0145-FEDER-007638 (FCT Ref. UID/AMB/50017/2013), financed by national funds through the FCT/MEC and co-financed by FEDER under the PT2020 Partnership Agreement.

References

Amand, L.-E., Bo, L., Lücke, K., Werther, J., 2001. Advanced air staging techniques to improve fuel flexibility, reliability and emissions in fluidized bed co- combustion. Stockholm.

Calvo, A.I., Tarelho, L.A.C., Alves, C.A., Duarte, M., Nunes, T., 2014. Characterization of operating conditions of two residential wood combustion appliances. Fuel Processing Technology 126, 222–232. doi:http://dx.doi.org/10.1016/j.fuproc.2014.05.001

Carbon Trust, 2009. Biomass heating: a practical guide for potential users, second. ed. London.

Carvalho, R.L., Vicente, E.D., Tarelho, L.A.C., Jensen, O.M., 2018. Wood stove combustion air retrofits: A low cost way to increase energy savings in dwellings. Energy and Buildings 164, 140–152. doi:https://doi.org/10.1016/j.enbuild.2018.01.002

Castillo, T., Guillén, J., Moquera, L., Rivadeneira, T., Segura, K., Yujato, M., 2017. Anuario 2017 de Estadísticas Energéticas, Primera. ed. OLADE, Quito - Ecuador.

Chin, K.L., H'ng, P.S., Paridah, M.T., Szymona, K., Maminski, M., Lee, S.H., Lum, W.C., Nurliyana, M.Y., Chow, M.J., Go, W.Z., 2015. Reducing ash related operation problems of fast growing timber species and oil palm biomass for combustion applications using leaching techniques. Energy 90, 622–630. doi:https://doi.org/10.1016/j.energy.2015.07.094

Dagwa., I.M., Ibhadode., A.O., 2008. Some physical and mechanical properties of palm kernel shell (PKS). Botswana Journal of Technology 17. doi:http://dx.doi.org/10.4314/bjt.v17i2.52206

Danielsen, F., Beukema, H., Burgess, N.D., Parish, F., Brühl, C.A., Donald, P.F., Murdiyarso, D., Phalan, B., Reijnders, L., Struebig, M., Fitzherbert, E.B., 2009. Biofuel Plantations on Forested Lands: Double Jeopardy for Biodiversity and Climate. Conservation Biology 23, 348–358. doi:10.1111/j.1523-1739.2008.01096.x

Garcia-Nunez, J.A., Garcia-Perez, M., Rodriguez, D.T., Ramirez, N.E., Fontanilla, C.A., Stockle, C., Amonette, J.E., Frear, C.S., Silva Lora, E.E., 2015a. Evolution of palm oil mills into biorefineries: Technical and enviromental assesment of six biorefinery options, in: Biorefinery I: Chemicals and Materials from Thermo-Chemical Biomass Conversion and Related Processes.

Garcia-Nunez, J.A., Ramirez-Contreras, N.E., Rodriguez, D.T., Silva Lora, E.E., Frear, C.S., Stockle, C., Garcia-Perez, M., 2015b. Evolution of palm oil mills into bio-refineries: Literature review on current and potential uses of residual biomass and effluents. Resources, Conservation and Recycling 110, 99–114. doi:http://dx.doi.org/10.1016/j.resconrec.2016.03.022

Garcia-Nunez, J.A., Rodriguez, D.T., Fontanilla, C.A., Ramirez, N.E., Silva Lora, E.E., Frear, C.S., Stockle, C., Amonette, J., Garcia-Perez, M., 2016. Evaluation of alternatives for the evolution of palm oil mills into biorefineries. Biomass and Bioenergy 95, 310–329. doi:http://dx.doi.org/10.1016/j.biombioe.2016.05.020

Heredia, M.A., Tarelho, L.A.C., Matos, A., Robaina, M., Narváez, R., Peralta, M.E., 2018. Thermoeconomic analysis of integrated production of biochar and process heat from quinoa and lupin residual biomass. Energy Policy 114, 332–341. doi:https://doi.org/10.1016/j.enpol.2017.12.014

Honorable Congreso Nacional, 2016. Código del trabajo. Registro Oficial Suplemento 167, Ecuador.

Honorable Congreso Nacional, 2014. Ley orgánica de régimen tributario interno. Registro Oficial Suplemento 463, Ecuador.

Instituto Nacional de Eficiencia Energética y Energías Renovables, 2018. Consumos Energéticos Invisibles: el caso de la Industria. Revista Científica del Desarrollo Energético 8–11.

Koh, L.P., Wilcove, D.S., 2008. Is oil palm agriculture really destroying tropical biodiversity? Conservation Letters 1, 60–64. doi:http://doi.wiley.com/10.1111/j.1755-263X.2008.00011.x

Loo, S. van, Koppejan, J., 2008. The Handbook of Biomass Combustion and Co-firing, Second. ed. Earthscan, London.

MAMAOT, 2013. Prevenção e controlo integrados da poluição. Diário da República, Portugal.

Masiá, A.A.T., Buhre, B.J.P., Gupta, R.P., Wall, T.F., Palm, B., 2007. Characterising ash of biomass and waste. Fuel Processing Technology 88, 1071–1081. doi:10.1016/j.fuproc.2007.06.011

Mendoza, M., 2014. Panorama preliminar de los subsidios y los impuestos a las gasolinas y diésel en los países de América Latina. CEPAL, Santiago de Chile.

Ministerio de Agricultura Ganadería Pesca y Acuacultura, 2014. Diagnóstico de la cadena de la palma aceitera, plan de mejora competitiva, in: Análisis Sectorial Aceite de Palma Y Elaborados. Quito, p. 18.

Ministerio de Electricidad y Energía Renovable, 2014. ATLAS Bioenergético de la República del Ecuador. Quito.

Mitschke, T., 2016. Desarrollo de análisis de mercado nacional e internacional de los productos de pellet. Quito.

Nilsson, D., Bernesson, S., Hansson, P.-A., 2011. Pellet production from agricultural raw materials – A systems study. Biomass and Bioenergy 35, 679–689. doi:10.1016/j.biombioe.2010.10.016

Ninduangdee., P., Kuprianov., V., 2014. Combustion of palm kernel shell in a fluidized bed: Optimization of biomass particle size and operating conditions. Energy Conversion and Management 85, 800–808. doi:http://dx.doi.org/10.1016/j.enconman.2014.01.054

Obaidullah, M., Dyakov, I. V., Thomassin, J.D., Duquesne, T., Bram, S., Contino, F., De Ruyck, J., 2014. CO emission measurements and performance analysis of 10 kW and 20 kW wood stoves. Energy Procedia 61, 2301–2306. doi:10.1016/j.egypro.2014.12.443

PETROECUADOR, 2018. Precios de venta a nivel de terminal para las comercializadoras [WWW Document]. URL http://www.eppetroecuador.ec/wp-content/uploads/downloads/2017/12/precios-enero-2018.pdf (accessed 3.25.18).

Pio, D.T., Tarelho, L.A.C., Matos, M.A.A., 2017. Characteristics of the gas produced during biomass direct gasification in an autothermal pilot-scale bubbling fluidized bed reactor. Energy 120, 915–928. doi:10.1016/j.energy.2016.11.145

Presidencia de la República, 2015. Reglamento sustitutivo para la regulación de los precios de los derivados de los hidrocarburos. Registro Oficial Suplemento 613, Ecuador.

Razuan, R., Chen, Q., Zhang, X., Sharifi, V., Swithenbank, J., 2010. Pyrolysis and combustion of oil palm stone and palm kernel cake in fixed-bed reactors. Bioresource Technology 101, 4622–4629. doi:10.1016/j.biortech.2010.01.079

Roundtable on Sustainable Palm Oil, 2013. Principles and Criteria for the Production of Sustainable Palm Oil [WWW Document]. Draft of Colombia´s National interpretation (NI) of the 2013 standard. URL https://rspo.org/publications/download/224fa0187afb4b7 (accessed 7.3.18).

Shackley, S., Hammond, J., Gaunt, J., Ibarrola, R., 2011. The feasibility and costs of biochar deployment in the UK. Carbon Management 2, 335–356. doi:10.4155/cmt.11.22

Tarelho, L.A.C., Ribeiro, J.P.S.P.O., E.R., T., Vicente, E.A.D., Matos, M.A.A., 2015. Residual forest biomass combustion in a pilot-scale bubbling fluidised bed: influence of fuel properties and characteristics of ashes produced, in: ETA-Florence Renewable Energies (Ed.), 23rd European Biomass Conference and Exhibition. EUBCE 2015, Vienna, pp. 745–757. doi:10.5071/23rdEUBCE2015-2BV.2.54

The engineering toolbox, 2018a. Higher and lower calorific values for some common fuels [WWW Document]. Fuels. URL http://www.engineeringtoolbox.com/specific-heat-solids-d_154.html

(accessed 2.20.18).

The engineering toolbox, 2018b. Altitude above sea level and air pressure [WWW Document]. Elevation and atmospheric pressure curves. URL https://www.engineeringtoolbox.com/air-altitude-pressure-d_462.html (accessed 1.3.18).

The European Commission, 2015a. The European Commission, implementing Directive 2009/125/EC of the European Parliament and of the Council with regard to ecodesign requirements for solid fuel boilers. Official Journal of the European Union, European Union.

The European Commission, 2015b. Implementing Directive 2009/125/EC of the European Parliament and of the Council with regard to ecodesign requirements for solid fuel local space heaters. Official Journal of the European Union, European Union.

Uemura, Y., Omar, W.N., Tsutsui, T., Yusup, S.B., 2011. Torrefaction of oil palm wastes. Fuel 90, 2585–2591. doi:10.1016/j.fuel.2011.03.021

Vassilev, S. V., Baxter, D., Andersen, L.K., Vassileva, C.G., 2010. An overview of the chemical composition of biomass. Fuel 89, 913–933. doi:10.1016/j.fuel.2009.10.022

Villada, J.L., Fuertes, F., Vaca, C., Cárdenas, D., 2016. El contexto energético del Ecuador. Análisis de oportunidades de I+D+i en eficiencia energética y energías renovables en Ecuador 15–31.

Zeng, T., Pollex, A., Weller, N., Lenz, V., Nelles, M., 2018. Blended biomass pellets as fuel for small scale combustion appliances: Effect of blending on slag formation in the bottom ash and pre-evaluation options. Fuel 212, 108–116. doi:10.1016/j.fuel.2017.10.036

Zeng, T., Weller, N., Pollex, A., Lenz, V., 2016. Blended biomass pellets as fuel for small scale combustion appliances: Influence on gaseous and total particulate matter emissions and applicability of fuel indices. Fuel 184, 689–700. doi:http://dx.doi.org/10.1016/j.fuel.2016.07.047

Nomenclature

Abbreviations

KS	Kernel shell
USD	United States dollars
LHV	Lower heating value
Y	Years
t	Tons
D	Diameter
L	Lenght
W	Width
AFR	Air fuel ratio
CE	Combustion efficiency

Subscripts

db	Dry basis
wb	Wet basis
stoich	Stoichiometric

Symbols		Units
wt%	Weight percentage	%
$W_{C,F}$	Carbon content in the fuel	$kg_C/kg_{,F}$

$W_{H,F}$	Hydrogen content in the fuel	$kg_H/kg_{,F}$
$W_{S,F}$	Sulfur content in the fuel	$kg_S/kg_{,F}$
$W_{O,F}$	Oxygen content in the fuel	$kg_O/kg_{,F}$
$W_{N,F}$	Nitrogen content in the fuel	$kg_N/kg_{,F}$
$W_{Z,F}$	Ash content in the fuel	$kg_Z/kg_{,F}$
M_C	Molar mass of Carbon	kg/mol
M_H	Molar mass of Hydrogen	kg/mol
M_O	Molar mass of Oxygen	kg/mol
M_N	Molar mass of Nitrogen	kg/mol
M_S	Molar mass of Sulfur	kg/mol
M_{H2O}	Molar mass of water	kg/mol
W_s	Stoichiometric oxygen	kg_{O2}/kg_{KS}
$Y_{s,C}$	Stoichiometric carbon	kg_C/kg_{KS}
$Y_{s,H}$	Stoichiometric hydrogen	kg_H/kg_{KS}
$Y_{s,S}$	Stoichiometric sulfur	kg_S/kg_{KS}
$W_{s,A}$	Stoichiometric air	kg_{air}/kg_{KS}
$Y_{s,O}$	Stoichiometric coefficient	$kmol_{O2}/kmol_{O2}$
$Y_{s,N}$	Stoichiometric coefficient	$kmol_{N2}/kmol_{O2}$
Y_{H2O}	Stoichiometric coefficient	$kmol_{H2O}/kmol_{O2}$
$W_{a,A}$	Combustion air	kg_{air}/kg_{KS}
z	Air excess	%

λ	Lambda coefficient	-
M_{air}	Molar mass of air	kg/mol
n_{CO2}	CO_2 yield in the flue gas	$kmol/kg_{KS}$
n_{H2O}	H_2O yield in the flue gas	$kmol/kg_{KS}$
n_{O2}	O_2 yield in the flue gas	$kmol/kg_{KS}$
n_{SO2}	SO_2 yield in the flue gas	$kmol/kg_{KS}$
n_{N2}	N_2 yield in the flue gas	$kmol/kg_{KS}$
C	Overall costs	USD/y
I_0	Initial investments costs	USD/y
CF	Cash flow	USD/y
S_f	Fuel cost savings	USD/y
S_{CO2}	Revenues due to CO_2 emissions trading	USD/y
D_c	Depreciation rate	%
I_t	Income tax	%
Ps_t	Profit sharing tax	%
OC	Operational costs	USD/y
FCF	Free cash flow	USD/y
PP	Payback period	y
OI	Operational income	USD/y
$EBTD$	Earnings before taxes and depreciation	USD/y

Highlights (3-5 bullet points)

- In relation to diesel, fuel costs could be reduced 8 times by the use of KS as fuel
- The amount of tax incentives equals to 57.7% of the combustion system capital costs
- The combustion efficiency during the steady state periods is 99.8%
- The CO concentration (260.1 mg/Nm^3) was below the emissions limit of 500 mg/Nm^3
- Ash sintering had a significant influence in the combustion process